Luminescent supramolecular heterometallic macrocycles and their encapsulation on cholate gels

Raquel Gavara,[a,*] Javier Mateos,[a] Ferran Sabaté,[a] Raquel Belda,[b,c] José Miguel Llinares,[b] Enrique García-España,[b,*] Laura Rodríguez[a,d,*]

[a] *Departament de Química Inorgànica i Orgànica, Secció de Química Inorgànica, Universitat de Barcelona, Martí i Franquès 1-11, 08028 Barcelona, Spain.*

[b] *Instituto de Ciencia Molecular (ICMOL), Departaments de Química Inorgànica i Orgánica, Facultat de Química, Universitat de València, Paterna. (Spain).*

[c] *Department of Chemistry, Durham University, South Road, Durham, DH1 3LE (UK.)*

[d] *Institut de Nanociència i Nanotecnologia (IN²UB). Universitat de Barcelona, 08028 Barcelona (Spain).*

E-mail: raquel.gavara@qi.ub.es, enrique.garcia-es@uv.es, laura.rodriguez@qi.ub.es.

Abstract

The metal complex formed by coordination of Zn(II) to 1,7-bis(4-methylpyridine)-4-(2-naphthylmethyl)-1,4,7-triazaheptane (**ZnL^{2+}**) was reacted in aqueous solution with [Pd(NO$_3$)$_2$(en)] and [Pt(NO$_3$)$_2$(en)] salts to form the self-assembled heterometallic macrocycles **[Zn$_2$L$_2$Pd$_2$(en)$_2$]$^{8+}$** and **[Zn$_2$L$_2$Pt$_2$(en)$_2$]$^{8+}$**, respectively. Pd(II) and Pt(II)-coordination modulates the original emission of **ZnL^{2+}** arising from the presence of the naphthalene chromophore and the formation of the macrocycles can be monitored due to the PET process occurring with coordination of Pd(II) and Pt(II) to the pyridine units of **ZnL^{2+}**. Additionally, several studies reveal that these heteromacrocycles can be encapsulated in Zn(II)-cholate hydrogels giving rise to soft materials with tunable emissive properties. Preliminary analysis show also that the addition of the metallic species in micromole concentration to the cholate hydrogels resulted in an improved mechanical strength of the final materials.

Keywords: metallomacrocycles; self-assembly; luminescence; cholate hydrogels; rheology.

Introduction

Supramolecular metallomacrocycles[1] and related supramolecular architectures[2-4] have attracted great attention on the last decades and 2D metallocycles with different geometries (such as triangles, squares, pentagons and hexagons) have been synthesized.[5,6] Several potential applications have been reported for these metallomacrocycles such as reactor cavities, catalysts, sensors, photonic devices and platforms for the design of materials with tailored properties, among others. In concrete, heterometallic supramolecular macrocycles where the second metal can introduce additional functionality and complexity to the final architectures are of special interest. In that sense, the use of Pt(II) and Pd(II) as second metal centers to be coordinated to pyridine moieties and related ligands has been very profitable[6-8]. This is mainly due to the structural diversity of pyridyl-based ligands, the geometry of the metal centers and the facility for tuning the lability of the coordination bond.

The use of this kind of supramolecular macrocycles in applications for daily life requires their supporting on a solid-like phase. A versatile approach involves the encapsulation in supramolecular gels. The latter are well known soft materials that are formed via non-covalent interactions of small molecules.[9] These interactions enable the reversible formation of large self-assemblies or supramolecular polymers, forming a solid-like network (minor component) which is able to entrap either an organic solvent or water (major component) through surface tension or capillary forces.[10] Due to their particular properties, in the last decades the use of supramolecular gels has been studied in a wide range of applications such as drug delivery and tissue engineering,[11,12] crystallization of pharmaceuticals,[13] luminescent materials,[14] reaction vessels and reusable catalysts,[15] and pollutant removal[16], among others.

Within this context, it is known that the interaction between the cholate anions and divalent or trivalent metal cations is able to form a 3D-netwotk which entraps water forming supramolecular hydrogels.[17,18] It is believed that the mechanism of gelation is related to metal-carboxyl cholate coordination, hydrogen bonding between cholate molecules and a delicate hydrophilic-hydrophobic balance.[17] The employment of trivalent lanthanides as metal cations has allowed the development of emissive soft materials with tunable luminescence.[18-21] Other applications for divalent-cholate

hydrogels have been reported such as their use as precursors for the development of lithium-based batteries.[21]

In this paper, we report the formation of heterometallic macrocycles through the interaction of a Zn(II)-polyamine complex with Pd(II) and Pt(II) species. The encapsulation of these macrocycles in Zn(II)-cholate hydrogels yields soft materials with tunable emission and improved mechanical properties.

Results and discussion

Formation of heterometallic macrocycles with ZnL^{2+}

Polyamine ligand 1,7-bis(4-methylpyridine)-4-(2-naphthylmethyl)-1,4,7-triazaheptane (**L**) that contains two N-donor groups at terminal positions (Figure 1) was reacted with a Zn(II) salt and subsequently with square planar [M(en)](NO$_3$)$_2$ (M = Pd^{2+}, Pt^{2+}) complexes in order to synthesize luminescent water soluble heterometallic macrocycles, taking advantage of the affinity of the pyridine moieties towards Pt(II) and Pd(II) cations. The intrinsic luminescent properties of **L** were very useful to follow the self-assembly processes (see below).
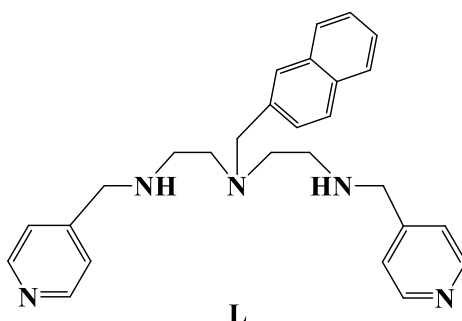

Figure 1. N-donor ligand used for the synthesis of metallomacrocycles.

Compound **L** was previously described[22] and consists of a triamine chain functionalized at both terminal positions with 4-picolyl units and at the central nitrogen with a methylnaphthyl fragment. It was observed that zinc(II) coordinates to the polyamine chain giving rise to the formation of **ZnL^{2+}** (Figure 2) which promotes the presence of a luminescence pH window by an "off - on - off" activity. The highest emission of **ZnL^{2+}** is observed at around pH 8. This is due to the fact that at higher pH values (pH > 7.9) a photoinduced electron transfer (PET) phenomenon occurs from the amine lone pair to the π - π* excited state of the naphthalene, quenching the emission of the signaling unit. On the other hand, at lower pH values (pH < 7.9) PET process also occurs, but in this case from the π–π* excited state of the naphthalene to the protonated pyridinium unit.[23,24] It is necessary to adjust the pH at around 7.9 in order to succeed with the synthesis of the corresponding macrocycles. In this way, amine groups are coordinated to the Zn^{2+} cation being a very useful situation to avoid competition with N-

4

pyridyl atoms in the coordination with Pt(II) and Pd(II) in the self-assembly process (Figure 2).[22,25]
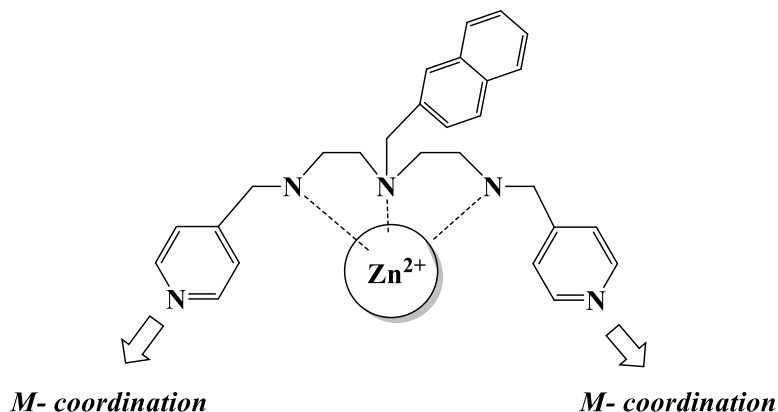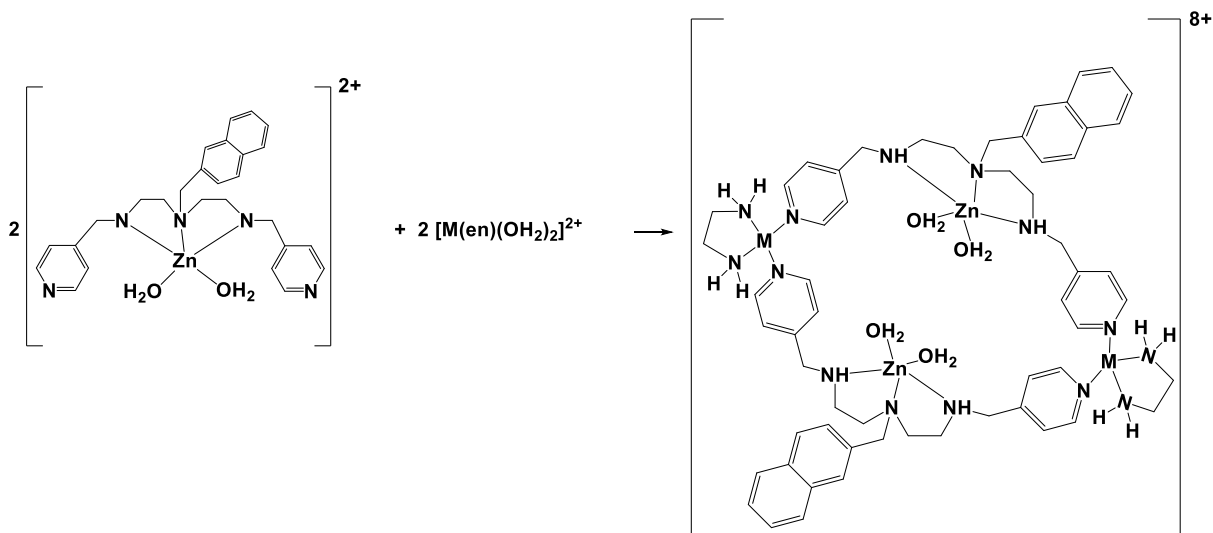

Figure 2. Schematic representation of **ZnL^{2+}** metalloligand suitable for M-pyridyl coordination.

Thus, the **ZnL^{2+}** complex was reacted with the [M(en)(H$_2$O)$_2$](NO$_3$)$_2$ (M = Pd, Pt) salt in water at the aforementioned pH value, in order to construct heterometallic macrocyclic structures by direct self-assembly reactions (Scheme 1).

Scheme 1. Synthesis of Zn/M (M = Pd, Pt) water soluble heterometallacycles in water at pH = 7.9.

The formation of the metallomacrocycles was carried out under spectroscopical conditions in water and followed by absorption and emission titrations. In this way, different amounts of a solution of [M(en)(H$_2$O)$_2$](NO$_3$)$_2$ were added to a solution of

ZnL^{2+} (5x10^{-5} M) and changes on the spectroscopical properties were followed at each point. Variations on the absorption spectra are mainly focused on the pyridyl unit with an increase of intensity at *ca*. 260 nm (Figure S1 in SUPPORTING INFORMATION). Moreover, the addition of the increasing amounts of Pd(II) or Pt(II) complex causes a decrease on fluorescence intensity of the naphthalene at *ca*. 335 nm (Figure 3) and reaches a plateau after the addition of *ca*. 2 equivalents Pd(II) or Pt(II) salt, being indicative of the formation of the expected supramolecular macrocycle. The decrease on the fluorophore's emission implies the activation of a quenching process. These changes in emission and absorption are analogous to those produced by protonation of pyridyl units[22] and suggest that the nitrogen atom of the aromatic amine could be coordinated to the square planar complex giving rise to the formation of heterometallic macrocycle (Scheme 1). Association constant values (Table 1) were calculated using the HypSpec 1.1.33 software for Windows[26] and in both cases, the system fits well to the formation of the 2+2 complex taking place in two steps:

$$2A + B \xrightleftharpoons{\quad K_1 \quad} A_2B \qquad \text{(eq. 1)}$$

$$A_2B + B \xrightleftharpoons{\quad K_2 \quad} A_2B_2 \qquad \text{(eq. 2)}$$

where A refers to the **ZnL^{2+}** complex and B to the heavy metal species, Pd(II) or Pt(II) respectively. It can be seen in Table 1, that whereas the formation of the A$_2$B complex is equally favoured for both heavy metal species, the formation of the 2:2 complex is easier in the case of Pd(II), as expected for the kinetically easier formation of Pd(II)-pyridyl bond.[27]
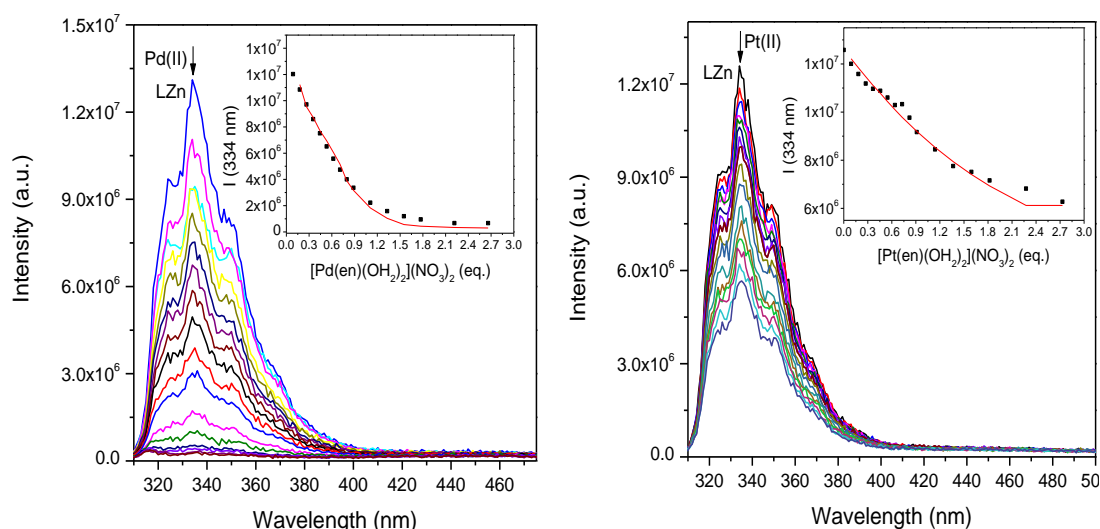
6

Figure 3. Emission spectra of **ZnL^{2+}** (λ_{exc} = 285 nm) in the presence of increasing amounts of [Pd(en)(H$_2$O)$_2$](NO$_3$)$_2$ (left) and [Pt(en)(H$_2$O)$_2$](NO$_3$)$_2$ (right). The inset shows the experimental intensity at the emission maximum (black squares) and the fitting curve (red line) calculated with HypSpec program from the equilibrium constants reported in Table 1.

Table 1. Association constants related to the formation of the 2:2 heterometallic macrocycles.

Reaction	Log K_1	Log K_2
2A + B ⇌ A$_2$B (A = **ZnL^{2+}**; B = Pd(II))	7.82 ± 0.02	7.04 ± 0.03
A$_2$B + B ⇌ A$_2$B$_2$ (A = **ZnL^{2+}**; B = Pt(II))	7.81 ± 0.01	4.40 ± 0.01

Additional MALDI-TOF MS experiments were performed using the same concentrations and controlled pH that in the titration experiments. Peaks assigned to the adducts {L$_2$Zn$_2$[Pt(en)]$_2$(H$_2$O)$_8$(NO$_3$)$_5$}$^{3+}$ (m/z = 647.6), {L$_2$Zn$_2$[Pt(en)]$_2$(H$_2$O)$_9$(NO$_3$)$_5$}$^{3+}$ (m/z = 654.0) and {L$_2$Zn$_2$[Pt(en)]$_2$(H$_2$O)$_6$(NO$_3$)$_6$}$^{2+}$ (m/z = 984.5) were detected as a confirmation of the successful self-assembled macrocycle formation (Figure S2 in SUPPORTING INFORMATION) .

Encapsulation of the metallomacrocycles in cholate hydrogels

The production of emissive cholate hydrogels has been extensively studied in the last years.[28] Concerning this aspect, we have decided to synthesize cholate hydrogels

containing our emissive heterometallic complexes embedded within the supramolecular structure. In this way, hybrid supramolecular (cholate/metal complexes) gels can be obtained.

Cholate hydrogels were obtained by mixing $Zn(NO_3)_2 \cdot 6H_2O$ and sodium cholate in two different concentrations (30 mM/60 mM and 5 mM/10 mM, respectively), Figure 4. The same procedure was followed for the formation of the hybrid structures containing **$[Zn_2L_2M_2(en)_2]^{8+}$** (M = Pt, Pd) and **ZnL^{2+}** metalloligand in micromole concentration (see Experimental Section for details), in order to obtain luminescent hybrid matrices and compare their photophysical and rheological properties (Figure 5).
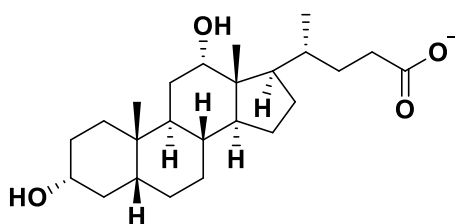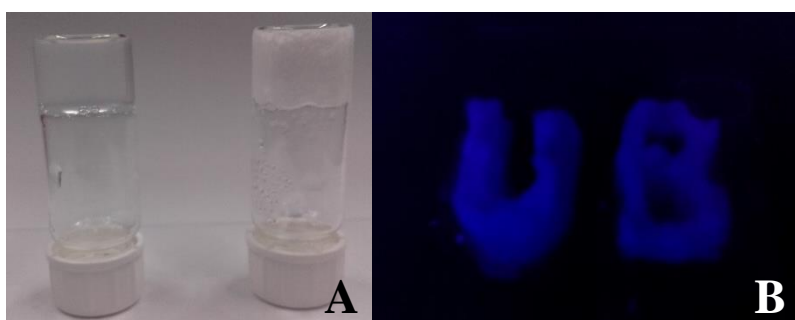

Figure 4. Structure of cholate anion.

Figure 5. A) Cholate hydrogel containing Zn(II) as gelation agent in 5/10 mM conditions (left) and 30/60 mM and small amounts of **$[Zn_2L_2Pt_2(en)_2]^{8+}$**; B) Luminescent hydrogel containing a small amount of **$[Zn_2L_2Pt_2(en)_2]^{8+}$** in 30/60 mM conditions (Zn:cholate)

Preliminary studies show that conversely to the pure Zn(II)-cholate hydrogel, the inclusion of micromolar amounts of L metal complexes ease the gelation process and no sonication is necessary in these cases. Thus, the metal complexes have an important effect on the supramolecular assemblies and it must interact with the cholate fibers during the supramolecular entanglement.

8

Optical microscopy (OM) between crossed polarizers and electronic microscopy (TEM) were used to analyze in more detail the structure of these gels (Figures S3 and S4 in SUPPORTING INFORMATION). These techniques revealed that the presence of metalloligand and heterometallic species (ZnL^{2+}/$[Zn_2L_2Pd_2(en)_2]^{8+}$/$[Zn_2L_2Pt_2(en)_2]^{8+}$) gives rise to a higher entanglement than in the parent cholate gel, and in the case of $[Zn_2L_2Pd_2(en)_2]^{8+}$ and $[Zn_2L_2Pt_2(en)_2]^{8+}$ samples, also wider fibers were observed.

Rheology experiments were performed with our gels and the obtained parameters are summarized in Table 2. Frequency sweep experiments at a constant stress of 1 Pa were carried out on these gels at a constant temperature of 25 ºC.

Table 2. Rheological data of Zn^{2+}-cholate hydrogel and corresponding hydrogels doped with metallic (1.5×10^{-6} M) species from frequency sweep experiments, at 1 Pa constant stress (G' and G'' values measured at a frequency of 10.0 Hz; error ± 10-15%).

Encapsulated species	G' (Pa)	G'' (Pa)	σ* (Pa)	G'/G''
-	2277	465	50	4.9
ZnL^{2+}	8253	1168	-	7.0
$[Zn_2L_2Pd_2(en)_2]^{8+}$	12480	1819	-	6.9
$[Zn_2L_2Pt_2(en)_2]^{8+}$	10315	1399	-	7.4

As displayed in Figure 6, the storage modulus (G') is more than 3-fold higher in the presence of the ZnL^{2+} metalloligand and increases in a factor of 4 and 6 (4- or 6-fold) in the presence of the metallosupramolecular species $[Zn_2L_2Pd_2(en)_2]^{8+}$ and $[Zn_2L_2Pt_2(en)_2]^{8+}$, respectively. The loss moduli (G'') also increases in the presence of the metal complexes, but in lower extension, as seen in Table 2. Thus, the calculated G'/G'' ratio is higher in the presence of ZnL^{2+}, $[Zn_2L_2Pd_2(en)_2]^{8+}$ and $[Zn_2L_2Pt_2(en)_2]^{8+}$, indicating that low concentrations of these species are able to improve the mechanical properties of the cholate hydrogel[29,30] which seems to be slightly favorable in the case of the $[Zn_2L_2Pt_2(en)_2]^{8+}$. Additionally, in the used measurement conditions, the yield stress value (σ*) could be only detected for the blank Zn(II)-cholate gel, an additional indication of the lower strength of this sample. The role

of the metallosupramolecular species in the improvement of the mechanical strength of the gels is currently under investigation.
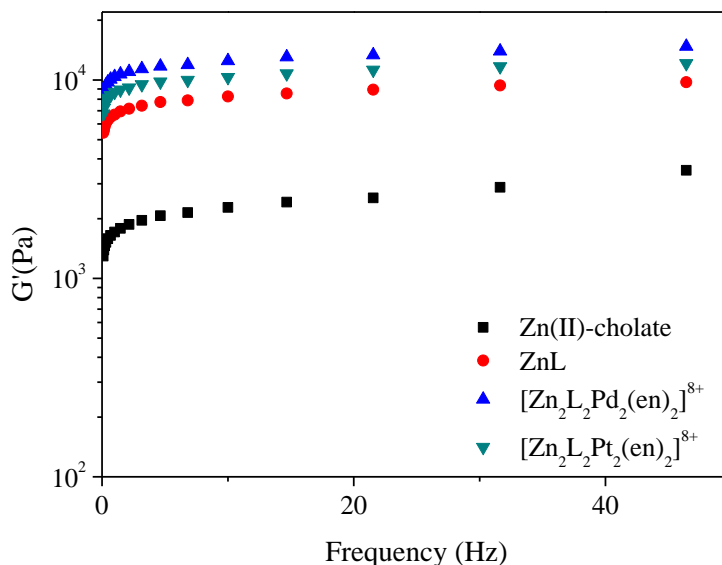

Figure 6. Comparison of storage moduli from frequency sweep experiments of Zn^{2+}-cholate gel and same gel containing $\mathbf{ZnL^{2+}}$, $\mathbf{[Zn_2L_2Pd_2(en)_2]^{8+}}$ and $\mathbf{[Zn_2L_2Pt_2(en)_2]^{8+}}$ ($c = 1.5 \times 10^{-6}$ M) at 1 Pa constant stress.

Emission properties of the cholate gels

The inclusion of metallic complexes gives rise to luminescent hydrogels. The emission spectra of **30/60** cholate gels after addition of increasing amounts of $\mathbf{ZnL^{2+}}$, $\mathbf{[Zn_2L_2Pd_2(en)_2]^{8+}}$ and $\mathbf{[Zn_2L_2Pt_2(en)_2]^{8+}}$ show an increase of luminescence due to the presence of the naphthalene chromophore (Figure S5-S7). This observable fact presents the same trend as in aqueous solutions, being $\mathbf{ZnL^{2+}}$ the most emitting gel and $\mathbf{[Zn_2L_2Pd_2(en)_2]^{8+}}$ the least (Figure 7). As commented above, the quenching of the $\mathbf{ZnL^{2+}}$ emission in the presence of the heavy atom salts is attributed to the formation of metallomacrocycles involving the coordination of Pd(II) or Pt(II) to the pyridyl units. This gives rise to a photoinduced electron transfer process from the $\pi-\pi^*$ excited state of the naphthalene to the pyridyl moieties.[22,31,32] The reason for the higher quenching in the case of Pd(II) in front of Pt(II) is not clear, although higher quantum yields have been reported for other Pt(II) complexes by comparison with their Pd(II) analogues.[33,34]

10

Thus, the formation of the gel using Zn^{2+} cation as gelator base does not influence too much the naphthalene emission in the organic matrix. These measurements also point out that the metallic complexes involving **L** are maintained in the gel matrices. We should highlight that the introduction of the **ZnL^{2+}** and **[Zn$_2$L$_2$M$_2$(en)$_2$]$^{8+}$** (M = Pt, Pd) doping agents at micromolar concentration are able not only to ease the gelation and strength of the matrix but also to introduce luminescent properties. This fact opens the possibility to obtain new luminescent materials that can be used as portable luminescent sensors for the in situ detection of specific guests.
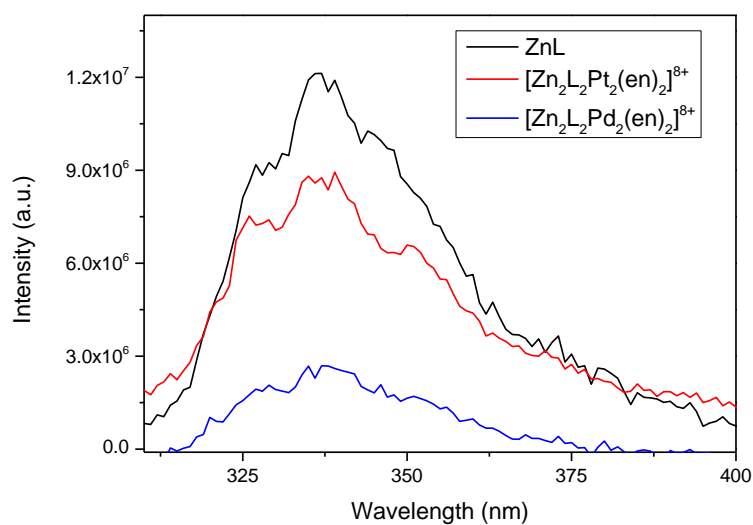

Figure 7. Emission spectra of **ZnL^{2+}**, **[Zn$_2$L$_2$Pd$_2$(en)$_2$]$^{8+}$** and **[Zn$_2$L$_2$Pt$_2$(en)$_2$]$^{8+}$** (c = 3.5x10^{-6} M) embedded within cholate hydrogels (λ_{exc} = 285 nm).

11

Conclusions

The metal complex comprising Zn(II) and the ligand 1,7-bis(4-methylpyridine)-4-(2-naphthylmethyl)-1,4,7-triazaheptane is able to interact with Pd(II) and Pt(II) salts to form heteromacrocyclic structures, as pointed out by fluorescence and absorption titrations. The employment of the metallosupramolecular species at micromolar concentration as additives in Zn(II)-cholate hydrogels, gives rise to materials with emissive properties. Additionally, preliminary analysis show that the inclusion of the metallosupramolecular species in the cholate matrices is responsible for the formation of wider fibers as well as a higher entanglement of the solid-like network, as observed by microscopy techniques and rheology analysis.

12

Experimental Section

General information

All compounds were synthesized under pre-purified nitrogen atmosphere using standard Schlenk under inert atmosphere. The solvents used in the synthetic procedures were purified by a Puresolve (Innovative Technologies) solvent purification and kept under nitrogen. Polyamine ligand **L**[22] and metal salts [Pd(NO$_3$)$_2$(en)] and [Pt(NO$_3$)$_2$(en)] were prepared as previously reported.[35]

Physical Measurements

Absorption spectra were recorded on a Cary 100 scan 388 Varian UV-spectrophotometer and emission spectra on a Horiba-Jobin- Yvon SPEX Nanolog spectrofuorimeter. MALDI-TOF MS measurements were performed in a Applied Biosystems 4700 Proteomics Analyzer 2011. Optical micrographs were recorded with a Leica DM1000LED and TEM images with a Tecnai G2 Spirit.

Rheological measurements were performed in an ARES7 rheometer (Rheometric Scientific) using a plate-plate geometry with 1 mm gap and at a constant temperature of 25°C. Dynamic frequency sweep measurements were performed in the linear viscoelastic regime (1 Pa stress), which was previously determined by dynamic strain sweep measurements.

Spectrophotometric and Spectrofluorimetric titrations

Titrations for the synthesis of heterometallic Zn(II)/Pd(II) or Zn(II)/Pt(II) macrocycles have been carried out at 25 °C in air-equilibrated water by addition of aliquots of $2 \cdot 10^{-3}$ M solution of the corresponding platinum and palladium salt to a $5 \cdot 10^{-5}$ M solution of polyamine ligand at pH 8 after addition of an equimolar amount of a concentrated solution of ZnCl$_2$ to form the 1:1 Zn/**L** complex. The pH has been controlled after addition of each aliquot of Pd or Pt salt. The association constants of the complexes with the anions have been obtained from the fit of the spectrophotometric or fluorimetric titrations data with HypSpec 1.1.33 software for Windows.[26]

Preparation of cholate hydrogels

13

A variable amount of ZnL^{2+}, $[Zn_2L_2Pd_2(en)_2]^{8+}$ and $[Zn_2L_2Pt_2(en)_2]^{8+}$ solutions, giving a concentration in the final mixture between 0 and 3.5 μM, was mixed with 1.5 mL of $Zn(NO_3)_2 \cdot 6H_2O$ (30 or 5 mM) in a 5 ml glass vial and the pH was adjusted to 8 using NaOH 0.1M and HCl 0.1M solutions. Then, 1.5 mL of sodium cholate (60 or 10 mM) was added at room temperature. For mixtures $Zn(NO_3)_2$/sodium cholate 30/60 mM, sonication during 25-30 gave rise to white gels. In the case of $Zn(NO_3)_2$/sodium cholate 5/10 mM mixtures, transparent gels were obtained and no sonication was required in the case of mixtures containing the metalloligand ZnL^{2+} and heterometallic species $[Zn_2L_2Pt_2(en)_2]^{8+}$, $[Zn_2L_2Pd_2(en)_2]^{8+}$.

Acknowledgments

Supporting Information Available

Absorption spectra corresponding to the titrations of ZnL^{2+} with Pd(II) and Pt(II) salts; OM images between cross-polarizers corresponding to the blank Zn(II)-cholate hydrogel and the same matrix doped with ZnL^{2+}, $[Zn_2L_2Pt_2(en)_2]^{8+}$ and $[Zn_2L_2Pd_2(en)_2]^{8+}$ species; TEM images between corresponding to the blank Zn(II)-cholate hydrogel and the same matrix doped with ZnL^{2+}, $[Zn_2L_2Pt_2(en)_2]^{8+}$ and $[Zn_2L_2Pd_2(en)_2]^{8+}$ species; Emission spectra of Zn(II)-cholate hydrogel doped with different amounts of ZnL^{2+}, $[Zn_2L_2Pt_2(en)_2]^{8+}$ and $[Zn_2L_2Pd_2(en)_2]^{8+}$ species.

14

[1] H. Amouri, C. Desmarets, J. Moussa, *Chem. Rev.* **2012**, *112*, 2015–2041, and references cited therein.

[2] H. Soudry, C. Desmarets, G. Gontard, T. Edgington, A. L. Cooksy, H. Amouri, *Dalton Trans.* **2017**, *46*, 10240-10245.

[3] L. Mimassi, C. Guyard-Duhayon, L. Raehm, H. Amouri, *Eur. J. Inorg. Chem.* **2002**, 2453-2457.

[4] C. Desmarets, I. Azcarate, G. Gontard, H. Amouri, *Eur. J. Inorg. Chem.* **2011**, 4558–4563.

[5] Y.-Y. Zhang , W.-X. Gao, L. Lin, G.-X. Jin, *Coord. Chem. Rev.* **2017**, *344*, 323–344, and references cited therein.

[6] M. D. García, C. Alvariño, E. M. López-Vidal, T. Rama, C. Peinador, J. M. Quintela, *Inorg. Chim. Acta* **2014**, *417*, 27–37, and references cited therein.

[7] S. Leininger, B. Olenyuk, P. J. Stang, *Chem. Rev.* **2000**, *100*, 853-908.

[8] X. Yan, T. R. Cook, P. Wang, F. Huang, P. J. Stang, *Nat. Chem.* **2015**, *7*, 342–348.

[9] D. B. Amabilino, D. K. Smith, J. W. Steed, *Chem. Soc. Rev.* **2017**, *46*, 2404–2420.

[10] X. Huang, P. Terech, S. R. Raghavan, R. G. Weiss, *J. Am. Chem. Soc.* **2005**, *127*, 4336-4344.

[11] K. J. Skilling, F. Citossi, T. D. Bradshaw, M. Ashford, B. Kellam, M. Marlow, *Soft Matter.* **2014**, *10*, 237-256.

[12] C. A. Angulo-Pachón, D. Navarro-Barreda, C. M. Rueda F. Galindo, J. F. Miravet, *J. Colloid Interface Sci.* **2017**, *505*, 1111-1117.

[13] L. Kaufmann, S. R. Kennedy, C. D. Jones, J. W. Steed, Chem. Commun. 2016, 52, 10113-10116.

[14] Z. Zhao, J. W. Y. Lam, Ben Zhong Tang, *Soft Matter* **2013**, *9*, 4564-4579.

[15] D. Díaz Díaz, D. Kühbeck, R. J. Koopmans, *Chem. Soc. Rev.* **2011**, *40*, 427–448.

[16] O. B. Okesola, D. K. Smith, *Chem. Soc. Rev.* **2016**, *45*, 4226-4251.

[17] Y. Qiao, Y. Lin, Z. Yang, H. Chen, S. Zhang, Y. Yan, J. Huang, *J. Phys. Chem. B* **2010**, *114*, 11725–11730.

[18] S. Bhowmik, S. Barnejee, U. Maitra, *Chem. Commun.* **2010**, *46*, 8642-8644.

[19] S. Banerjee, R. Kandanelli, S. Bhowmik, U. Maitra, *Soft Matter*, **2011**, *7*, 8207–8215.

[20] R. Laishram, S. Bhowmik, U. Maitra, *J. Mater. Chem. C* **2015**, *3*, 5885-5889.

[21] G. Ma, Y. Zhang, J. Lin, Z. Chen, R. Zhao, P. Tong, L. Zou, H. Chen, *J. Solid State Electrochem.* **2015**, *19*, 3365–3372.

[22] R. Aucejo, J. Alarcón, E. García-España, J. M. Llinares, K. L. Marchin, C. Soriano, Carlos Lodeiro, M. A. Bernardo, F. Pina, J. Pina, J. Seixas de Melo*, Eur. J. Inorg. Chem.* **2005**, 4301-4308.

[23] A. P. de Silva, H. Q. N. Gunaratne, T. T. Gunnlaugsson, A. J. M. Huxley, C. P. McCoy, J. T. Rademacher, T. E. Rice, *Chem. Rev.* **1997**, *97*, 1515–1566.

[24] A. P. de Silva, S. Uchiyama, *Molecular Logic Gates and Luminescent Sensors Based on Photoinduced Electron Transfer* in *Luminescence Applied in Sensor Science*, Eds. L. Prodi, M. Montalti, N. Zaccheroni, 2011, Springer-Verlag Berlin Heidelberg.

[25] C. Bravin, E. Badetti, F. A. Scaramuzzo, G. Licini, C. Zonta, *J. Am. Chem. Soc.* **2017**, *139*, 6456-6460.

[26] P. Gans, A. Sabatini, A. Vacca, *Talanta* **1996**, *43*, 1739-1753.

[27] M. Ferrer, A. Pedrosa, L. Rodríguez, O. Rossell, M. Vilaseca, *Inorg. Chem.* **2010**, *49*, 9438–9449

[28] N. M. Sangeetha and U. Maitra, *Chem. Soc. Rev.* **2005**, *34,* 821–836.

[29] R. Kandanelli, A. Sarkar, U. Maitra*, Dalton Trans.*, **2013**, *42*, 15381-15386.

[30] A. Chakrabarty, U. Maitra, A.D. Das, *J. Mater. Chem.*, **2012**, *22*, 18268-18274.

15

[31] C. Monnereau, J. Gomez, E. Blart, F. Odobel, *Inorg. Chem.* **2005**, *44*, 4806-4817.

[32] M. Zhang, M. L. Saha, M. Wang, Z. Zhou, B. Song, C. Lu, X. Yan, X. Li, F. Huang, S. Yin, P. J. Stang, *J. Am. Chem. Soc.* **2017**, *139*, 5067−5074.

[33] D. Xu, H.J. Murfee, W.E. Van der Veer, B. Hong, *J. Organomet. Chem.* **2000**, *596*, 53-63.

[34] M. Ferrer, L. Rodríguez, O. Rossell, *J. Orgnomet. Chem.* **2003**, *681*, 158-166.

[35] A. Orita, L. S. Jiang, T. Nakano, N. C. Ma, J. Otera, *Chem. Commun.* **2002**, 1362-1363.

Click here to access/download

Supporting Information

Supporting_Information_revised.doc

Graphical Abstract

Click here to access/download
Additional Material - Author
Graphical_Abstract.doc